Mansoura University
Faculty of Engineering
Mansoura Engineering Journal

# Development and Investigation of the Performance of a New Self-Aspirated Microbubbles Generator

# تطوير وبحث أداء مولد فقاعات متناهية الصغر يعمل بالتهوية الذاتية

Ali M. Aboghazala, *Ayman I. Bakry*, Aly H. Gadallah and EL-Shenawy A. EL-Shenawy

**KEYWORDS:**
**Microbubbles, microbubbles generator, coanda effect, water aeration**

***الملخص العربي*:- في هذا البحث تم تصميم وتصنيع مولد جديد لانتاج فقاعات متناهية الصغر من خلال حدوث كل من السريان الدوامى وسريان كوندا فى نهاية حافة مخرج البوق, التى تجعل الفقاعات الكبيرة تتفتت الى فقاعات صغيرة جدا. بدلا من التكلفة العالية لأنظمة الهواء المضغوط لعملية توليد الفقاعات يتم سحب الهواء الجوى ذاتيا وذلك بسبب تكون ضغط سالب كبير من الفتحة الموجوده فى عنق الخنق فى البوق. تغطى هذه الدراسة كوندا بنصف قطر (0 و20 مم) ومعدل سريان ماء 21.4 لتر/ الدقيقة, ومعدل سريان هواء من 0.1 إلى 0.9 لتر/ الدقيقة . وقد أظهرت النتائج مدى متوسط الأقطار الصغيرة جدا تتراوح بين 64.3 الى 87.6 ميكرومتر ، وأن قطر الفقاعة يقل بزيادة نصف قطر الكوندا وانخفاض معدل السريان الحجمى للهواء.**

***Abstract*—In this research, a new bubble generator to produce fine bubbles was designed and manufactured through the interaction between a strong swirl and coanda flow at the edge of an exit nozzle, a larger bubble could be breakdown into fin microbubbles. A significant vacuum pressure was created at the throat of the exit nozzle to induce the atmospheric air required for bubbles generation process replacing high cost compressed air systems. This study covered coanda radius (0 and 20 mm), water flow rates 21.4 l/min and air flow rates 0.1 to 0.9 l/min. The results indicate, fine average diameter range between 64.3 to 87.6 µm depending on air flow rates and coanda radius. Bubble diameter decreases with increasing coanda radius and reducing the induced air flow rate.**

*Received: 9 October, 2016 - revised: 6 November, 2016 - accepted: 20 November, 2016*

*Ali M. Aboghazala, demonstrator at Tanta University, Faculty of Engineering, Mechanical Power Dept., Egypt*

*Ayman I. Bakry, Associate professor at Tanta University, Faculty of Engineering, Mechanical Power Dept., Egypt*

*Aly H. Gadallah, Lecturer at Tanta University, Faculty of Engineering, Mechanical Power Dept., Egypt*

*EL-Shenawy A. EL-Shenawy, professor at Tanta University, Faculty of Engineering, Mechanical Power Dept., Egypt*

## I. INTRODUCTION

MICROBUBBLE is defined as an extremely small bubble, that can be uniformly suspended in liquid [1]. Li et al. [2] defined the microbubbles as the bubbles with diameters of several tens of micrometers and having some characteristics which are different from larger bubbles in the millimeter's range.

Microbubbles have large surface area per unit volume and less effect on floating force, which makes it to use better in water treatment technology [3]. In the medical field, microbubbles have been utilized as a contrast agent together with ultrasound to enhance visualization of blood flow [4]. Microbubbles have been used to separate oil from oil-polluted soil [5]. Kodama et al. [6] blew microbubbles at the bottom of large sized ship to reduce the frictional resistance between ship and water during navigation. Nakatake et al. [7] injected air microbubbles to the diesel fuel to improve the combustion of diesel engine

Recently most of the studies have shown that the rising velocity of microbubble follow the classical Stokes law serves as a guide for the residence time of a microbubble in a viscous

liquid [8]. The inside-outside pressure difference of a microbubble is very high as decreasing the bubble diameter, so the partial pressure of the dissolving gas increases that increases the gas dissolution. Due to this high pressure inside the bubble, gas inside the microbubbles tends to diffuse outside from a region of high pressure to a low pressure of surrounding., the microbubbles shrink and finally collapse, causing high mass transfer rate of gas microbubble to the surrounding liquid [9].

For conventional generation of ordinary bubbles, nozzles or orifices are often used. Fine bubbles are usually produced using porous media, constant flow nozzles, or membrane. However, it is hard to generate microbubbles using these techniques due to the difficulty of preventing bubble coalescence. For this reason, microbubbles are often generated by different ways that can be divided into their mechanism. Pressurization type uses the sudden pressure drop to form Microbubbles. Because of reduction in pressure, the supersaturated air is released into expelled water in the form of microbubbles. Measurements of bubble sizes for the pressurization type indicate that microbubbles maintain a steady diameter range of 10 to 100 μm with an average diameter between 40 and 80 μm [10, 11]. Fujiwara [12, 13] generated about 100 μm size bubble by using Venturi system, pump forces pressurized fluid into the venture tube, an increase in velocity occurs in the throat part simultaneously with the decrease in pressure which leads to air being sucked in through the tube, the sucked gas bubbles collapse yielding small bubbles as pressure recover takes places further downstream. Ejector type uses the venturi effect of a converging–diverging nozzle to convert the pressure energy of a motive fluid to velocity energy which creates a low-pressure zone that draws in and entrains a suction gas. After passing through the throat of the injector, the gas–liquid mixer expands and the velocity is reduced [14]. Ohnari [15] developed a cylindrical microbubble generator by pumping water from the tangential direction, when the fluid takes air out of the generator with very high rotating velocity, air can be sheared into microbubbles.

The Coanda effect is defined as the tendency of a fluid to adhere to an adjacent surface, placed sideways to the jet itself [16]. In the field of aeronautical engineering, it can be used to increase the lift of an airplane during taking off and aiming at decreasing the taking off distance [17].

Harumichi et al. [18] developed a micro bubbles generator in which the water flow is channelized into a swirl pattern by guided vanes. An air compressor is used to deliver air into the center of guided vanes to produce fine bubbles.

In this research, to overcome the high cost of compressed air systems, a new bubble generator including a swirl pattern by guided vanes, breakdown nozzle connected coaxially to each other and coanda flow at the edge of an exit nozzle, to produce fin bubbles was achieved. The pressurized water flow is channelized into a swirl pattern by guided vanes swirler, which sequentially causes a reduction in pressure in its central axial part. The present proposed micro bubbles generator is basically similar to the one developed by Harumichi et al. [18] with the advantage of eliminating the need for compressed air system. A significant vacuum pressure was created at the throat of the exit nozzle to induce the atmospheric air for coanda radius 20 mm. Finally, the air - water mixture then develops microbubbles due to high turbulent mixing and shearing mechanism.

## II. EXPERIMENTAL SETUP

A schematic diagram and photographic view of the experimental setup constructed for this study are shown in Fig.1. (a, b). It consists of the main glass tank arrangement, the microbubbles generator (MBG) arrangement and the optical measuring arrangement.

Water is pumped in a closed loop via a centrifugal pump into a bubbles generator arrangement and a main glass tank arrangement as shown in Fig. 1. The pump (MATRA-CD70NT) is driven by a 3-phase motor. It has a maximum output power of 2.25 kW at a maximum running speed of 2800 rev/min. The pump can be able to produce a pressure of 7 bar at an optimum flowrate of 40 l/min when running at its maximum speed. The water flowrate is regulated to any required value by varying the pump speed between zero and the maximum rating speed of motor via an electronic inverter (Eurotherm Drives, 650/022/400). It is measured through a water flow meter (HAOYU Electronics, FS300A G3/4"). It has a maximum reading of 60 l/min and an accuracy of ± 3 %. The flow rate readings are monitored through a self-made data logger system. The flow meter is calibrated by measuring a known volume of water with the time. For each flowrate, the corresponding consumed power by the motor is measured by a power meter (Ram, JYA.CZ1.16).

The water is concentrically conducted to the upstream connector of the bubbles generator arrangement as shown in Fig.2. It passes firstly throughout the spaces between long circumferential blades of a swirler made of PLA material. It is manufactured using a 3-D print technology. It has an overall length of 70 mm, an outer diameter of 56 mm, and a constant blades height of 7.5 mm. The swirler is designed to receive the water flow smoothly and free of shocks at its blades inlets. This is made through forming its frontal end on the shape of an axisymmetric half-paraboloid body, as shown in Fig. 2, and aligning its inlet blades angle coaxially. However, the water flow is continuously twisted along the blades block to produce a strong swirl flow at its exit section. In this study, the outlet blades angles are bent to make an angle of 70° with the axial direction of the arrangement. The swirler is mounted at 20 mm from the inlet section of a cylindrical acrylic tube of 57 mm in inner diameter and 140 mm in long.

Then, the resulting swirl water flow is secondly conducted to a special teflon nozzle that is manufactured on a turning machine as shown in Fig. 2. The inner surface of its upstream part is formed on the shape of a convergent nozzle with a profile due to the proposed equation by Morel [19]

$$\frac{D_x - D_2}{D_1 - D_2} = 1 - \frac{1}{X^2}\left(\frac{x}{L}\right)^3 \quad for\ \frac{x}{L} \le X$$

$$\frac{D_x - D_2}{D_1 - D_2} = \frac{1}{(1-x)^2}\left(1 - \frac{x}{L}\right)^3 \ for\ \frac{x}{L} \ge X$$

Where $D_x$ is the diameter at a distance $x$ from the inlet, $D_1$ is the nozzle inlet diameter, $D_2$ is the nozzle exit diameter, L is the nozzle length. A value of (X= 0.6) from the nozzle inlet section is selected in the present investigation to get the inverted point closer to the nozzle throat to reduce the pressure drop losses due to the strong swirl flow. The nozzle throat is of 7 mm in diameter and 105 mm in long. A hole of 1.5 mm in diameter is drilled 30 mm from the nozzle edge. It is connected to the air feeding system which is left opened to the atmospheric surrounding at its end for coanda radius 20 mm or attached to the compressed air lab system for coanda radius 0 mm depending on the pressure condition at the nozzle throat. The air flow rate is regulated through a fine needle valve positioned at the inlet of the air feeding system. It is monitored through a rotameter (Dewer, VFA-22-SS) with a maximum reading of 1 l/min and an accuracy of ± 2.5 %. The static pressure in the air feeding line is measured by a differential digital manometer (Extec, 407001A) with a maximum reading of ± 2000 mbar and a readability of ± 1 mbar. The inner surface of the downstream part of the nozzle is rounded, as shown in Fig. 2, to impose the Coanda effect onto the incoming accelerated swirl flow. In this study, two values of Coanda radius (0 and 20 mm) are manufactured and devoted as an independent parameter.

The bubbles generator arrangement is assembled to a side wall of a large 8 mm glass tank with dimensions of 750 mm × 550 mm × 260 mm as shown in Fig. 1. It is filled with filtered water up to a height of 450 mm. The drain from the tank is drawn into the pump through an opening located in the opposite position to the bubbles generator arrangement on the side wall. A hollow trapezoidal glass tank with the dimensions shown in Fig. 3. is mounted inside the main tank to confine the entire water flow to pass through a shallow passage of 30 mm in thickness where the test section is devoted for the purpose of optical measurements.

The shadowgraph technique (backlighting), as shown in Fig. 3, is used to measure the size and the size distribution of microbubbles. The technique is based on detecting the shadow from crossing illuminated bubbles confined within a specific illuminated area in the flow field on an imaging sensitive surface of high resolution. The illuminating source must be able to illuminate uniformly the complete predefined area of view. Also, it must be synchronized with the detecting imaging element to freeze the movement of the observed bubbles, as shown in Fig. 3. A pulsed laser beam (Double laser Nd: YAG laser, λ=532 nm) with special optics is used as an illuminating source for the test section where the optical measurements are carried out.

A Charge Coupled Device (CCD) camera (Lavison, 12bit, 1280*1024pixels, 8HZ) is applied as a detecting imaging medium. It is synchronized with the laser unit and both controlled through the CPU of the system. The entire operating parameters and data acquisition conditions of the system are identified and managed through a special software (Lavison, Geometry Package for Davis 6.2) [20]. In the present study, 150 consecutive images are taken for every set of operating parameters. The recorded images are constantly saved on storage media for further post processing procedures. The figure of this number seems fairly larger than the 90 images to obtain a good enough convergent result for the ensemble mean diameter of the detected bubbles. In order to identify and then measure fine bubbles in micro scales, a special optical configuration should be attached in the preceding of the CCD camera. Many configurations for magnifying a specific tiny area in the flow field can be prepared. The one which is applied in the current study could be able to observe everything occurring in a very small area of 1.870 mm × 1.495 mm. This area is situated in a mid-way of the narrow passage between the main glass tank and the hollow trapezoidal glass tank as shown in Fig.3.

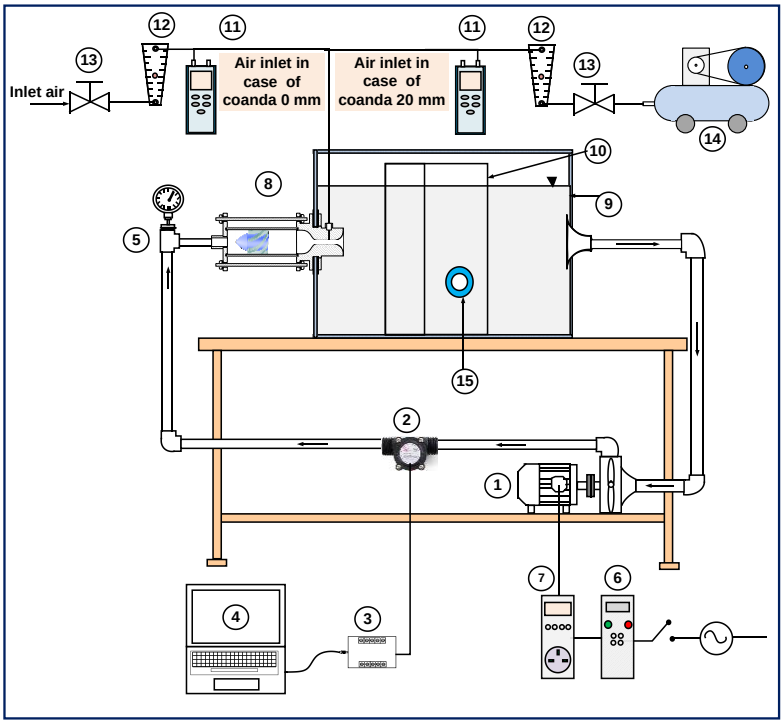


| | | | |
|---|---|---|---|
| 1 | Pump | 9 | Main glass tank |
| 2 | Water flow meter | 10 | Hollow trapezoidal glass tank |
| 3 | Data acquisition card | 11 | Air differential pressure manometer |
| 4 | Laptop | 12 | Air rotameter |
| 5 | Water pressure gauge | 13 | Accurate needle valve |
| 6 | Inverter | 14 | Air compressor |
| 7 | Power meter | 15 | Measuring optical arrangement |
| 8 | Microbubble generator arrangement | | |

Fig.1. (a) A schematic diagram of experimental set-u

Fig.1. (b) photograph for experimental set-up

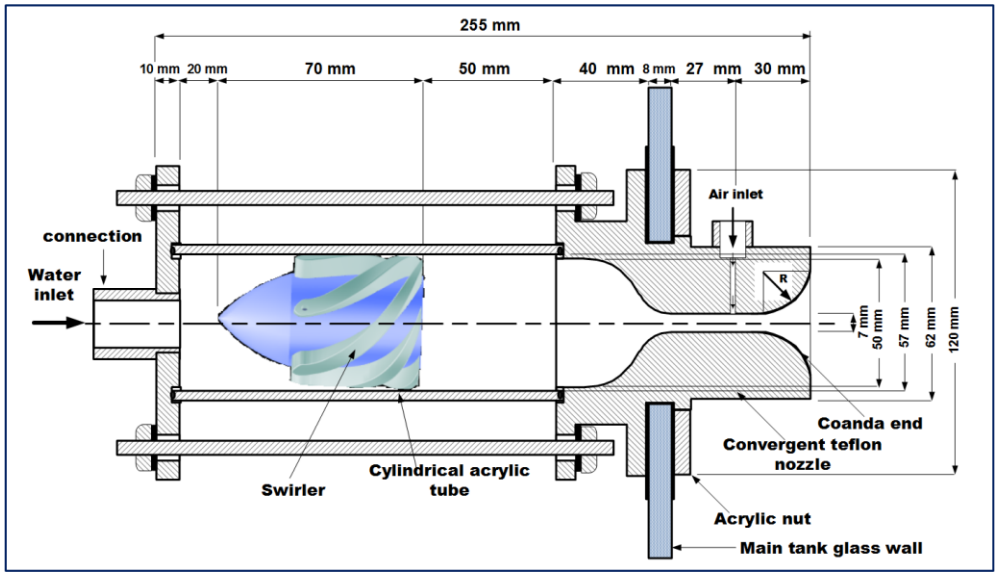


Fig. 2. Details of microbubbles generator arrangement

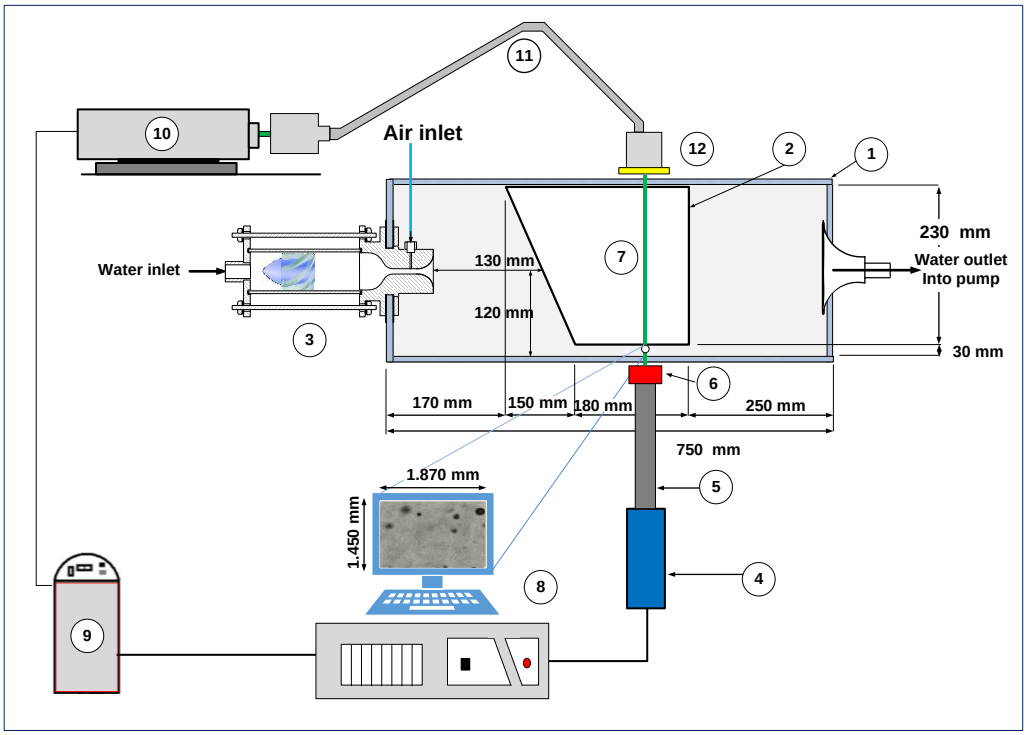


| | | | |
|---|---|---|---|
| 1 | Main glass tank | 7 | Laser beam |
| 2 | Hollow trapezoidal glass tank | 8 | CPU |
| 3 | Microbubble generator arrangement | 9 | Laser power supply |
| 4 | CCD camera | 10 | Double pulse Nd: YAG laser |
| 5 | Extension tube | 11 | Laser arm |
| 6 | Camera focus lenses | 12 | Fluorescence plate |

Fig.3. Optical measuring system

## III. RESULTS AND DISCUSSION

The results in this section are presented in the following sequence: initially, the size distribution of microbubbles produced by two cases of coanda effect, the variation of the measured pressure and power consumption of pump for different air and water flow rates.

### *3.1 Comparison of microbubbles size*

The size distribution of microbubbles produced by two different coanda radius (0 and 20 mm) are compared in Fig. 4. (a, b, c, d and e) At the air flow rates of (0.1, 0.3, 0.5, 0.7 and 0.9 l/min) respectively and water flow rate of 21.4 l/min. With ambient air temperature of 28 ºC.

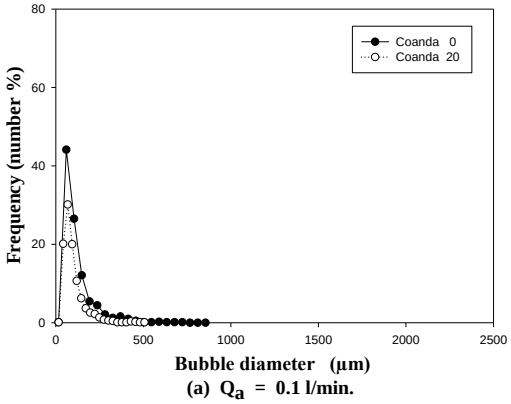


(a)

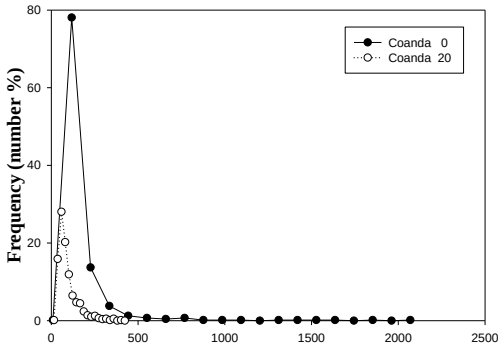


**(b) $Q_a$ = 0.3 l/min.**

(b)

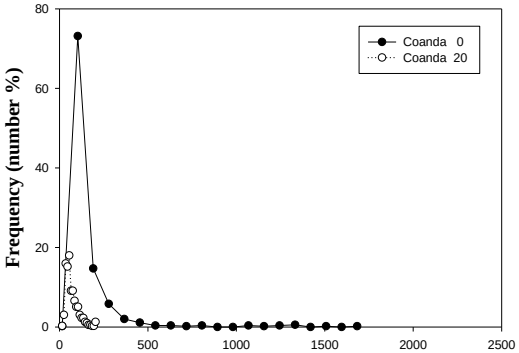


**(c) $Q_a$ = 0.5 l/min.**

(C)

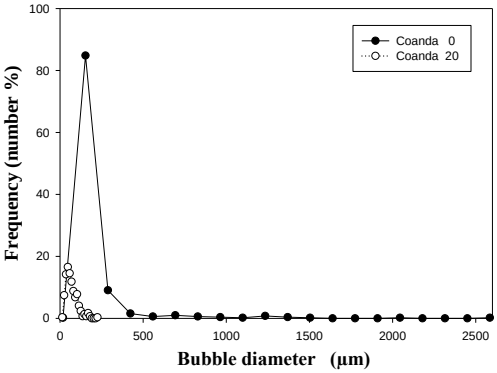


**(d) $Q_a$ = 0.7 l/min.**

(e)

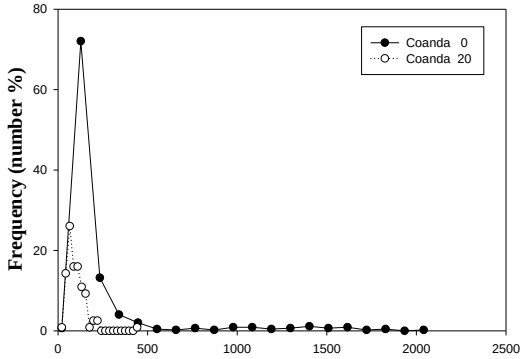


**(e) $Q_a$ = 0.9 l/min.**

Fig. 4.a,b,c,d &e
Histogram of bubble size distributions for coanda radius (0 and 20 mm) at Qw = 21.4 l/min.

Figure 4 shows the numerical frequency at each diameter rang. Bubbles generated by two different coanda radius (0 and 20 mm) under the present condition were mainly distributed in the range of 20 to 200 µm. Much smaller microbubbles were formed by the coanda radius 20 mm as compared to the coanda radius 0 mm. Microbubbles generated by coanda radius 0 mm have the broadest distribution and the largest mode diameter. The micro-bubbles are made from turbulence and strong shear stress at throat part.

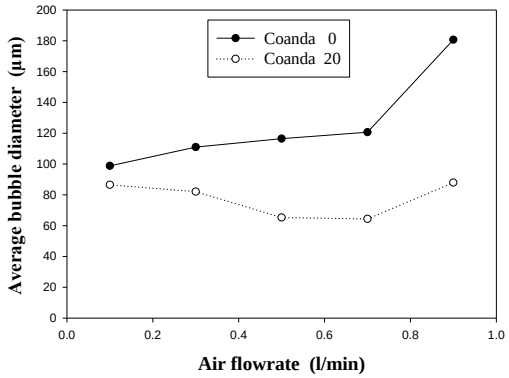


Fig. 5. Average bubble diameter generated by Coanda 0 and Coanda 20 at Qw = 21.4 l/min

The average diameter is shown in Fig.5. Microbubbles generated by coanda radius 20 mm have the smallest average diameter of 64.3 µm and 87.6 µm for Microbubbles generated by coanda radius 0 mm.

*3.2. Measured air pressure*

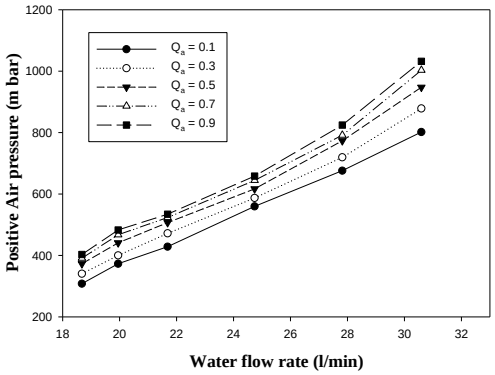


Fig. 6. Measured variation of Pressure and water flow rate, for coanda radius 0 mm.

Figure 6 shows the variations of the measured positive pressure delivering from air compressor and water flow rate range 18.5 to 31.5 l/min for coanda radius of 0 mm. The measured pressure increases with increasing water flow rate and air flow rate for coanda radius 0 mm.

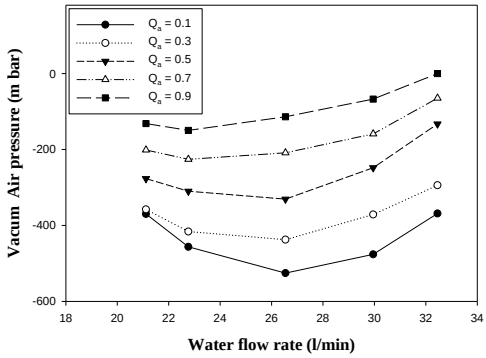


Fig. 7. Measured variation of Pressure and water flow rate, for Coanda radius 20 mm

Figure 7 shows the variations of the measured negative pressure and water flowrate range 21.4 to 33 l/min for coanda radius 20 mm. The vacuum pressure increases with decreasing the air flow rate. The maximum measured values of pressure are found for air volume flow rate 0.1 l/min. The combination of rotational and axial flow velocities in swirl flows gives distinctive features of induced air pressure. For low water flow rate, the tangential component greater than the axial component, so swirl number increases obviously making more induced air pressure. At high water flow rates the tangential component less than the axial component, so swirl number decreases and induced air pressure is decreased.

*3.3. Power consumption of pump*

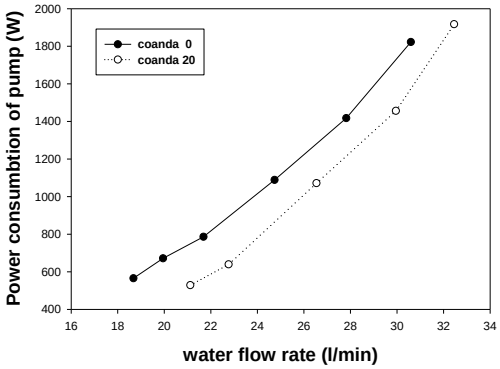


Fig. 8. The relation between power consumption and water flow rate of the pump

Figure 8 shows the variations of the measured power consumption of pump for two different coanda cases. The Friction drag of air-water two phase flow decreases with the decrease of microbubbles average diameter [6]. The measured power consumption of pump decreases for coanda radius 20 mm.

*3.4 Comparison with other micro bubbles generators*

Table 1 shows a comparison of the range of micro bubbles diameters produced by the present developed micro bubbles generator and the previous generators reported in the literature. It can be concluded that, the present generator is capable of producing micro bubbles with average sizes comparable to the previously developed generators without the need for compressed air system.

TABLE 1
METHODS OF MICROBUBBLES GENERATION

| **Method of microbubbles generation** | **Range of microbubbles diameters** |
|---|---|
| Rotary liquid flow type, Ohnari [21] | 10 - 50 µm |
| Static mixture type, Uematsu [14] | 5 - 50 µm |
| Venturi type, Fujiwara [13] | 100 µm |
| Ejector type, Nakatake et al. [7] | 40 - 50 µm |
| Ejector type, Sadatomi et al. [22] | 120 - 490 µm |
| swirl flow and coanda flow, This study | 64.3 - 87.6 µm |

## IV. CONCLUSIONS

Developed low power microbubble generator was investigated under two configurations of coanda effect. This study covered coanda radius (0 and 20 mm), water flow rates 21.4 l/min and air flow rates 0.1 to 0.9 l/min. Bubble diameter decreases significantly with increasing coanda radius and reducing the induced air flow rate. The results indicate, fine average diameter range 64.3 to 87.6 µm depending on air flow rates and coanda radius.

## NOMENCLATURE

| | |
|---|---|
| $Q_w$ | volumetric water flow rate, $m^3\ s^{-1}$ |
| $Q_a$ | volumetric air flow rate, $m^3\ s^{-1}$ |

## ABBREVIATIONS

| | |
|---|---|
| MBG | Microbubbles Generator |
| CCD | Charge Coupled Device |

## REFERENCES


[1] H. Tsuge, "Fundamental of microbubbles and nanobubbles," Bull Soc Sea Water Sci Jpn, vol. 64, pp. 4-10, 2010.

[2] P. Li, H. Tsuge, and K. Itoh, "Oxidation of dimethyl sulfoxide in aqueous solution using microbubbles," Industrial & Engineering Chemistry Research, vol. 48, pp. 8048-8053, 2009.

[3] P. Li and H. Tsuge, "Water treatment by induced air flotation using microbubbles," Journal of chemical engineering of Japan, vol. 39, pp. 896-903, 2006.

[4] J. R. Lindner, "Microbubbles in medical imaging: current applications and future directions," Nature Reviews Drug Discovery, vol. 3, pp. 527-533, 2004.

[5] Y. Tano, A. Iizuka, E. Shibata, and T. Nakamura, "Physical Washing Method for the Removal of Press Oil Using the High-Speed Movement of Microbubbles under Ultrasonic Irradiation," Industrial & Engineering Chemistry Research, vol. 52, pp. 15658-15663, 2013.

[6] Y. Kodama, A. Kakugawa, T. Takahashi, and H. Kawashima, "Experimental study on microbubbles and their applicability to ships for skin friction reduction," International Journal of Heat and Fluid Flow, vol. 21, pp. 582-588, 2000.

[7] Y. Nakatake, S. Kisu, K. Shigyo, T. Eguchi, and T. Watanabe, "Effect of nano air-bubbles mixed into gas oil on common-rail diesel engine," Energy, vol. 59, pp. 233-239, 2013.

[8] R. Parmar and S. K. Majumder, "Microbubble generation and microbubble-aided transport process intensification—A state-of-the-art report," Chemical Engineering and Processing: Process Intensification, vol. 64, pp. 79-97, 2013.

[9] H. OHNARI, "The characteristics and possibilities of micro bubble technology," Journal of MMIJ, vol. 123, pp. 89-96, 2007.

[10] S. E. De Rijk and J. G. den Blanken, "Bubble size in flotation thickening," Water Research, vol. 28, pp. 465-473, 1994.

[11] M. Han, Y. Park, J. Lee, and J. Shim, "Effect of pressure on bubble size in dissolved air flotation," Water Science and Technology: Water Supply, vol. 2, pp. 41-46, 2002.

[12] A. Fujiwara, S. Takagi, K. Watanabe, and Y. Matsumoto, "Experimental study on the new micro-bubble generator and its application to water purification system," in ASME/JSME 2003 4th Joint Fluids Summer Engineering Conference, 2003, pp. 469-473.

[13] A. Fujiwara, K. Okamoto, K. Hashiguchi, J. Peixinho, S. Takagi, and Y. Matsumoto, "Bubble breakup phenomena in a venturi tube," in ASME/JSME 2007 5th Joint Fluids Engineering Conference, 2007, pp. 553-560.

[14] H. Tsuge, Micro-and Nanobubbles: Fundamentals and Applications: CRC Press, 2014.

[15] H. ONARI, K. WATANABE, K. MAEDA, and K. MATSUO, "High functional characteristics of micro-bubbles and water purification," Resources processing, vol. 46, pp. 238-244, 1999.

[16] I. Reba, "Applications of the Coanda effect," Scientific American, vol. 214, pp. 84-92, 1966.

[17] F. Lalli, A. Bruschi, R. Lama, L. Liberti, S. Mandrone, and V. Pesarino, "Coanda effect in coastal flows," Coastal Engineering, vol. 57, pp. 278-289, 2010.

[18] H. Abe, K. Matsuuchi, and M. Iidaka, "Micro-bubble generator, vortex breakdown nozzle for micro-bubble generator, vane swirler for micro-bubble generator, micro-bubble generating method, and micro-bubble applying device," ed: Google Patents, 2011.

[19] T. Morel, "Comprehensive design of axisymmetric wind tunnel contractions," Journal of Fluids Engineering, vol. 97, pp. 225-233, 1975.

[20] "Software Manual,Version 6.1,by LaVison GmbH, Gottingen," 2001.

[21] H. Onari, "High Technology in Multiphase Flow: Waste Water Purification in Wide Water Area by Use of Micro-bubble Techniques," Japanese Journal of Multiphase Flow, vol. 11, pp. 263-266, 1997.

[22] M. Sadatomi, A. Kawahara, K. Kano, and A. Ohtomo, "Performance of a new micro-bubble generator with a spherical body in a flowing water tube," Experimental Thermal and Fluid Science, vol. 29, pp. 615-623, 2005..